

# Universal origin of unconventional $1/f$ noise in the weak-localization regime

C. Barone,<sup>1,2,\*</sup> F. Romeo,<sup>1,2</sup> A. Galdi,<sup>2,3</sup> P. Orgiani,<sup>2</sup> L. Maritato,<sup>2,3</sup> A. Guarino,<sup>1,2</sup> A. Nigro,<sup>1,2</sup> and S. Pagano<sup>1,2,†</sup>

<sup>1</sup>*Dipartimento di Fisica “E.R. Caianiello”, Università di Salerno, I-84084 Fisciano, Salerno, Italy*

<sup>2</sup>*CNR-SPIN, UOS di Salerno, I-84084 Fisciano, Salerno, Italy*

<sup>3</sup>*Dipartimento di Ingegneria dell’Informazione, Ingegneria Elettrica e Matematica Applicata, Università di Salerno, I-84084 Fisciano, Salerno, Italy*

(Received 2 August 2012; revised manuscript received 13 March 2013; published 17 June 2013)

The transport properties of manganite thin films characterized by a weak-localization transition have been studied. Detailed voltage noise measurements show a specific  $1/f$  noise spectrum below the transition temperature. A theoretical interpretation in terms of universal conductance fluctuations explains the nature of the unconventional electric noise, suggesting a direct connection between the weak-localization phenomenon and universal conductance fluctuations. The universal nature of the mechanism allows its detection in different systems under the weak-localization regime.

DOI: [10.1103/PhysRevB.87.245113](https://doi.org/10.1103/PhysRevB.87.245113)

PACS number(s): 72.15.Rn, 72.70.+m, 73.23.—b

## I. INTRODUCTION

Low-temperature electrical transport in a disordered metal is often influenced by quantum interference effects (QIEs) arising from the phase coherence of the electronic wave function over a distance  $L_\phi$  (i.e., the coherence length), which can be much longer than the elastic mean free path  $\ell$  at low temperatures or for large impurity concentration. One of these effects is weak localization (WL), a reduction of conductivity induced by the interference of phase coherent carriers backscattered from impurities. WL is revealed by an increase of resistivity at low temperature and by a peculiar magnetoresistance behavior, related to the phase shift induced by the magnetic field.<sup>1</sup>

An even more intriguing effect is the observation of universal conductance fluctuations (UCFs) in mesoscopic one-dimensional (1D) samples at very low temperatures (i.e., when the sample size  $L$  is  $\approx L_\phi$  and the transport is diffusive,  $L, L_\phi \gg \ell$ ). In such “small” systems, the interference between the electron trajectories determines a phase-dependent correction that does not average to zero and that depends on a specific impurity configuration. A magnetic field increment shifts the phases of the electrons, so that a different interference pattern results. This is seen in the magnetoresistance fluctuations, characterized at  $T = 0$  by a root-mean-square amplitude of  $\sim e^2/h$ , independent of sample size or degree of disorder.<sup>2,3</sup>

A direct connection between these two phenomena related to QIEs has been proposed but never demonstrated.<sup>4–6</sup> Indeed, WL is usually detected in systems of any dimensionality,<sup>1</sup> and at temperatures easy to access (in the range 10–80 K in oxides).<sup>7–9</sup> The UCF detection, instead, is limited to very peculiar sample geometry (i.e., nanowires, 1D-confined electron gases) and low temperature (typically 0.1–10 K).<sup>3,10</sup> In this respect, it is well known that the oscillations of the UCF magnetoresistance decay in large samples, due to ensemble averaging, and the amplitude of the fluctuations is reduced by the temperature increase, due to phase breaking excitations and energy level smearing. However, as already reported in the scientific literature,<sup>11–14</sup> the existence of UCFs can be probed in larger samples ( $L \gg L_\phi$ ) and at temperatures higher than 10 K by investigating temporal conductivity fluctuations characterized by a power spectral density of  $1/f$  type.

Electric noise spectroscopy, without the presence of an external magnetic field and with no limitation on operating temperatures, has proved to be a very sensitive method for studying the dynamic behaviors of the charge carriers and the kinetic processes in several systems, such as double perovskites,<sup>15</sup> manganites,<sup>16</sup> and electron-doped cuprate superconductors.<sup>7</sup> In these latter compounds, a preliminary study has revealed that WL gives rise to an unusual noise-spectral density of  $1/f$  type. In particular, under the WL regime the measured  $1/f$  noise shows a very weak temperature dependence and a peculiar *linear bias current scaling* of the spectral density  $S_V$ . At temperatures above the WL transition, the standard resistance fluctuation behavior is gradually recovered, yielding  $S_V \propto I^2$ .<sup>17</sup> This is evident in Fig. 1(a), where the experimental temperature and current dependencies of the voltage spectral density are shown in the case of  $\text{Nd}_{1.83}\text{Ce}_{0.17}\text{CuO}_{4+\delta}$  (NCCO) thin film samples, undergoing weak localization below a crossover temperature  $T_{\min} \sim 84$  K. In order to prove that this is not a peculiar behavior of NCCO compounds, a similar analysis has been performed on a different material, i.e.,  $\text{La}_{0.7}\text{Ba}_{0.3}\text{MnO}_3$  (LBMO) manganite. The experimental results are shown in Fig. 1(b) and qualitatively reveal the same dependence, although with a reduction of the crossover temperature of  $\sim 50$  K.

The aim of this paper is to explain the observed noise behavior, by identifying a universal origin of this phenomenon in terms of UCF induced noise. Due to the universal nature of the proposed mechanism, such phenomenology is expected to be relevant in low-dimensional systems where quantum corrections arise due to residual phase coherence. A model for the voltage noise spectral density based on the UCF physics is described in Sec. II. Section III contains the experimental results on LBMO thin films. In Sec. IV a discussion of the noise properties is addressed, also estimating the relevant energy scales involved in UCF processes. The conclusions are given in Sec. V.

## II. THEORETICAL FRAMEWORK

In disordered (macroscopic, i.e., of size  $L > L_\phi$ ) thin film systems at low temperature, the phase coherence of the sample over regions of typical size  $L_\phi$  may induce a

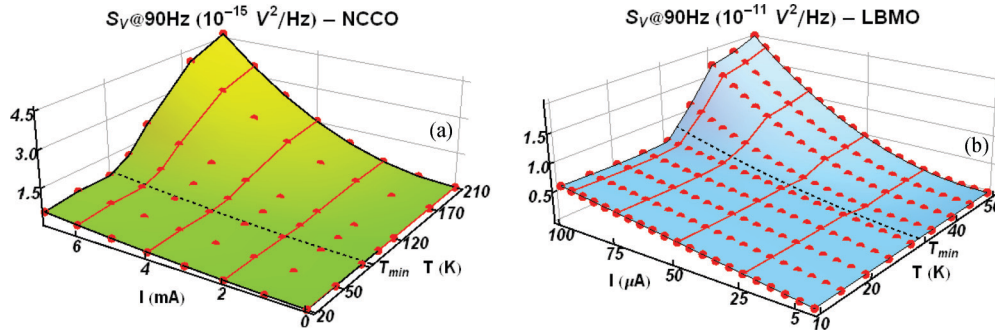


FIG. 1. (Color online) Temperature and bias current experimental dependencies of the  $1/f$  noise for  $\text{Nd}_{1.83}\text{Ce}_{0.17}\text{CuO}_{4+\delta}$  (a), and  $\text{La}_{0.7}\text{Ba}_{0.3}\text{MnO}_3$  (b) thin film samples. The two different crossover temperatures  $T_{\min}$ , below which WL effects occur, are shown with dashed lines. The  $S_V$  ranges are consistent with the resistance values, fulfilling the relation  $R_{\text{LBMO}}^2/R_{\text{NCCO}}^2 \sim 10^4$ .

noise based on the UCF phenomenology.<sup>11,18</sup> At  $T = 0$  the conductance of a metallic thin film is a sensitive function of the impurity configuration, and the alteration of even a single impurity over a sufficient distance may induce a conductance change of  $\approx e^2/h$ . At finite temperature, the sample is ideally divided into regions of typical size  $L_\phi < L$  within which coherence effects are relevant. The local vibration of impurities inside these coherent subsystems produces additive changes of the conductance variance, as long as the total variance of a single coherent subsystem  $\text{Var}[G_\phi]$  is saturated to the universal value  $\approx (e^2/h)^2$ ,  $G_\phi$  being the conductance of a single coherent subsystem.

For a disordered (diffusive) 2D metal (as the case of the samples reported here) characterized by  $L > L_\phi$  and diffusion constant  $\mathcal{D}$ , the Thouless energy  $E_c \sim h\mathcal{D}L_\phi^{-2}$  discriminates two electronic states from the interference viewpoint. Due to this, electronic states whose energy difference  $\delta E$  is less than  $E_c$  must be considered as indistinguishable from the interference viewpoint ( $\delta E \tau_D \sim \hbar$ ,  $\tau_D \approx L_\phi^2/\mathcal{D}$  being the finite lifetime) and thus can originate interference phenomena. On the other hand, electron waves fulfilling the condition  $\delta E > E_c$  are well separated in energy and thus their amplitudes must be added classically since interference phenomena become strongly suppressed. At given  $T$ , the relevant electronic processes occur within a given energy window  $\Delta E$  defined by the thermal energy  $k_B T$ . In the nonequilibrium condition, the coupling of the system with the external leads introduces a new energy scale  $eV_\phi$ , depending on the voltage  $V_\phi$  applied to the single coherent subsystem, so that  $\Delta E \sim \max[k_B T, eV_\phi]$ . According to this picture, the energy averaged  $\bar{G}_\phi$  over  $\Delta E$  fluctuates with a reduced variance given by

$$\text{Var}[\bar{G}_\phi] \sim \left(\frac{e^2}{h}\right)^2 \mathcal{N}^{-1}, \quad (1)$$

$\mathcal{N} = \Delta E \times E_c^{-1}$  being the number of uncorrelated energy intervals of size  $E_c$  contained in  $\Delta E$ . The variance of the conductance  $G$  of the whole system can be related to the variance of the single coherent subsystem using the relation

$$\text{Var}[G] \sim \left(\frac{L_\phi}{L}\right)^{4-d} \text{Var}[\bar{G}_\phi], \quad (2)$$

complemented by the conductance scaling law

$$G = (LL_\phi^{-1})^{d-2} \bar{G}_\phi, \quad (3)$$

where  $d = 2$  for a 2D film.<sup>19</sup> The quantity  $\text{Var}[G]/G^2$  is directly related to the observable noise through the integrated noise power

$$\frac{\text{Var}[G]}{G^2} = \int_{f_{\min}}^{f_{\max}} df \frac{S_V(f)}{V^2}. \quad (4)$$

For a  $1/f$  fluctuation the spectral power takes the form  $S_V(f) = \mathcal{A}f^{-1}$ , implying the equation

$$\frac{V^2}{G^2} \text{Var}[G] = f S_V(f) \ln\left(\frac{f_{\max}}{f_{\min}}\right), \quad (5)$$

where the frequency interval  $[f_{\min}, f_{\max}]$  is the experimental bandwidth. From the above arguments, one can recover the expression of the coefficient  $\mathcal{A}$  appearing in the spectral function in the form

$$\mathcal{A} = \frac{V^2}{G^2} \text{Var}[G] \frac{1}{\ln(f_{\max}/f_{\min})}. \quad (6)$$

At low temperature, typically below the characteristic crossover of QIE occurrence, the energy  $eV_\phi \approx \chi eIR$  (with  $\chi$  a dimensionless scaling parameter) provided by the external bias to a coherent subsystem is expected to be bigger than the Thouless energy  $E_c$ , thus constituting a relevant source of electronic dephasing. Compared to the thermal energy  $k_B T$ , the energy scale  $eV_\phi$  should dominate the low-temperature transport while, with increasing temperature and at low bias, the relation  $k_B T \gtrsim eV_\phi$  should be verified. Motivated by the experimental findings, it is possible to assume that the crossover between the usual behavior ( $\Delta E = k_B T$ ) and the bias-induced dephasing ( $\Delta E = eV_\phi$ ) occurs at temperatures close to  $T_{\min}$ .

The spectral density  $S_V(f)$  can be consequently written as ( $\Delta E > E_c$ )

$$S_V(f) = \mathcal{C} \left(\frac{e^2}{h}\right)^2 \frac{\tilde{E}_c \bar{G}_\phi^{-2}}{f \ln\left(\frac{f_{\max}}{f_{\min}}\right)} \times \begin{cases} (k_B T)^{-1} R^2 I^2, & T > T_{\min}, \\ (\chi e)^{-1} RI, & T < T_{\min}, \end{cases} \quad (7)$$

where  $\tilde{E}_c = (L_\phi L^{-1})^2 E_c$ , and the proportionality factor  $\mathcal{C}$  depends on the number of fluctuators inside the material. Equation (7) identifies the physical mechanism explaining, at low  $T$ , the anomalous linear dependence of the noise on the applied bias. The stochastic averaging of rms conductance  $\propto V^{-1/2}$  ( $V > V_c \equiv E_c/e$ ) has been confirmed in AuFe

spin-glass mesoscopic wires by Strunk *et al.*<sup>20</sup> The result in Ref. 20 has been obtained by using a theoretical argument similar to that here proposed, and by supposing the statistical independence of the electronic states separated by more than  $E_c$ . This assumption is strictly true only in one dimension, while in two dimensions it can be considered as a simplifying approximation to be validated *a posteriori*.

### III. EXPERIMENTAL RESULTS

Epitaxial LBMO thin films, where WL phenomena are likely to occur due to disorder,<sup>8,9</sup> have been prepared by pulsed laser deposition on SrTiO<sub>3</sub> (001) substrates, using low oxygen pressure ( $10^{-2}$  mbar) and low laser fluence (pulse energy 25 mJ).<sup>21</sup> While samples deposited at high fluence (200 mJ) are characterized by optimal transfer of target stoichiometry to the film and by an ordered microstructure, the samples under investigation are characterized by heavy ion (La, Ba) deficiency and by a disordered microstructure, with a consequent suppression of metal-insulator transition temperature  $T_{MI}$  from the bulk value.<sup>21</sup> However, the disorder induced by the fabrication technique does not lead to polycrystalline microstructures and preserves the epitaxial growth of the samples. Indeed, structural investigations have revealed the in-plane alignment among the LBMO unit cells, and a good in-plane matching and epitaxy between LBMO films and the substrate.

All the measurements were carried out in a closed-cycle cryocooler system, in a four-contacts configuration. The noise characterizations were performed using a low-noise dc current bias source and the resulting voltage was sent to a dynamic signal analyzer (HP35670A), through a low-noise preamplifier (PAR5113). The overall instrumental background noise was typically  $1.4 \times 10^{-17}$  V<sup>2</sup>/Hz. In order to rule out the existence of electrical noise generated by the contact probes, the experimental technique described in Ref. 22 was used.

The low-temperature dependence of resistivity of a typical LBMO sample is shown in Fig. 2, and is characterized by the

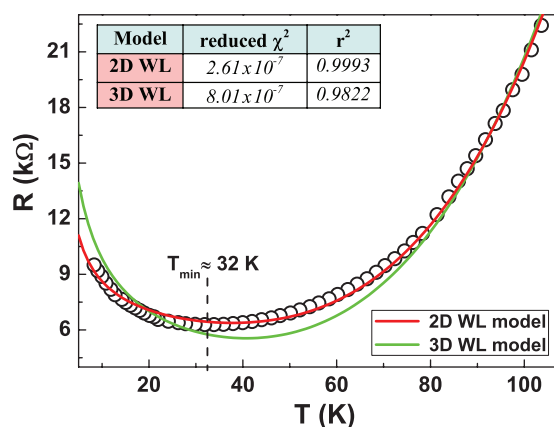


FIG. 2. (Color online) Low-temperature regime of resistivity for a typical LBMO investigated sample. The crossover temperature, corresponding with the resistance minimum, is  $T_{\min}$ . The red solid line represents the best fit to the experimental data points using Eq. (8), while the green curve corresponds to the best fit by using 3D WL  $[G_0 + C (T/T_0)^{p/2}]^{-1}$  correction to the low-temperature resistance behavior. In the inset are shown the  $\chi^2$  and  $r^2$  values.

presence of a low-temperature metal-to-insulator transition at  $T_{\min} \simeq 32$  K, likely due to the disorder appropriately induced. The  $R$  vs  $T$  data can be interpreted in terms of WL effects.<sup>1</sup> The best fit, with the lowest reduced  $\chi^2$  and highest coefficient of determination  $r^2$ , is obtained in the case of the 2D WL model, whose expression is

$$R(T) = \left[ G_0 + \frac{p}{2} \frac{e^2}{\hbar\pi^2} \ln\left(\frac{T}{T_0}\right) \right]^{-1} + AT^n, \quad (8)$$

where the second term is a contribution associated with a standard metal-like behavior. The good agreement between Eq. (8) and the experimental data is provided by the red solid line shown in Fig. 2. The best fit value for  $n$  ( $3.87 \pm 0.03$ ) is higher than 2, as usually occurs in disordered systems,<sup>23</sup> while  $p = (3.22 \pm 0.03)$  indicates electron-phonon interaction as the scattering mechanism.<sup>1</sup> An estimation of the quantity  $k_F \ell \approx 4.3$  is also made according to  $k_F \ell \approx \frac{\hbar}{e^2 R_{\min}}$ , where  $R_{\min}$  is the resistance value experimentally measured at  $T_{\min}$ .

The applicability of this quantum interference scenario to LBMO samples can be verified by performing  $R(T)$  measurements in an external magnetic field ( $H$ ). From the data in Fig. 3(a), it is clear that the application of  $H$  does not suppress the presence of the resistivity minimum. It is worth noting that, if the resistivity upturn would be due to intergranular tunneling (as is commonly observed in ceramic manganese samples), this minimum should gradually vanish under moderate  $H$ , while it should persist and be weakly affected by low  $H$  values in the case of quantum corrections to conductivity.<sup>24</sup> Alternatively, Coulomb interaction-driven localization can also originate a correction to  $R(T)$  of the form of Eq. (8) in 2D, even though in this case a positive magnetoresistance is expected,<sup>1</sup> contrary to the experimental behavior shown in Fig. 3(a).

These results, although not excluding the possibility of sample-specific minor transport processes, seem to exclude alternative mechanisms to WL as the dominant contribution to low-temperature transport (that is, grain boundary or Coulomb interaction effects). Conversely, the electrical conduction due to weak localization is compatible with the above arguments. In two dimensions the magnetic field dependence of the correction to the conductance due to weak localization is expressed as<sup>1</sup>

$$\delta G = G(H, T) - G(0, T) = \frac{e^2}{2\pi^2 \hbar} \left[ \Psi\left(\frac{1}{2} + \frac{1}{x}\right) + \ln(x) \right], \quad (9)$$

where  $\Psi(x)$  is the digamma function, and  $x = L_\Phi^2 4eH/\hbar$  (with  $L_\Phi$  the coherence length). Equation (9) has been compared with the experimental data of Fig. 3(a) and the resulting analysis is shown in Fig. 3(b). The agreement between the theoretical prediction (solid blue curve) and the data points (here reported at  $T = 30$  K) is clearly visible, while the only temperature-dependent fitting parameter  $L_\Phi$  has a value of 60 nm at 30 K. This is a semiquantitative estimation, as the temperature dependence of the WL correction cannot be entirely ascribed to the coherence length change with  $T$ . The reason is that nonuniversal aspects, such as the sample magnetic response, become relevant in complex magnetic materials,

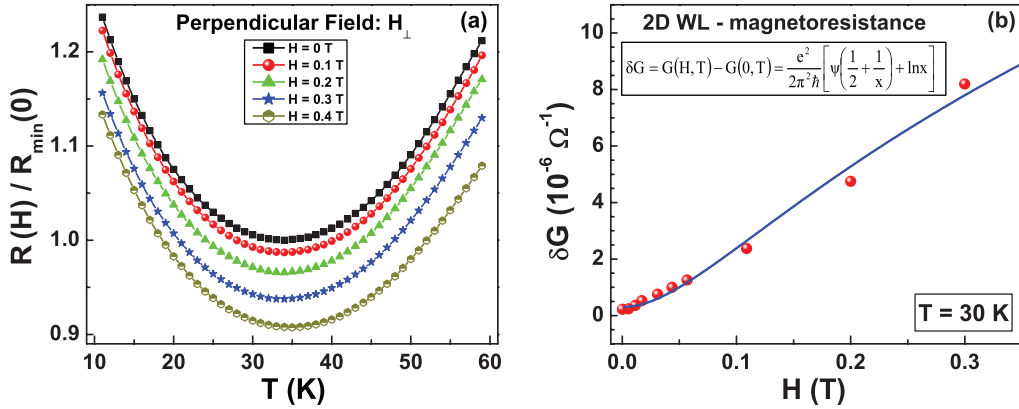


FIG. 3. (Color online) (a) Low-temperature dependence of the ratio  $R(H)/R_{\min}(0)$ ,  $R_{\min}(0)$  being the value of the resistance minimum at  $H = 0$ . An external magnetic field, ranging from 0 to 0.4 T, has been applied perpendicular to the in-plane easy axis of magnetization. (b) Magnetic field dependence of the weak-localization correction to the conductance. The experimental data points (red dots) are in a satisfactory agreement with the theoretical relation of Eq. (9) (solid blue curve).

while at fixed temperature the universal WL behavior can be recognized.<sup>25</sup>

Once the presence of WL corrections was confirmed, detailed characterization of the low-frequency (10–10<sup>4</sup> Hz bandwidth) voltage-noise  $S_V$  for several temperatures and bias currents was also performed. As shown in Figs. 4(a) and 4(c), the spectral density traces are characterized by an evident  $1/f^\gamma$  frequency dependence with  $\gamma = (1.02 \pm 0.03)$ . The background frequency-independent spectrum, corresponding to the sample Johnson noise and the electronic chain noise, is usually three to four orders of magnitude lower than the  $1/f$  component.

The temperature dependence of  $S_V$  reveals that fluctuation processes are essentially due to resistance at high temperatures. Conversely, the standard theory does not explain the noise below  $T_{\min}$ , where an upturn of the resistivity is observed. This unconventional characteristic of the  $1/f$  noise is evidenced by the bias current dependence of  $S_V$ , revealing a quadratic scaling of the spectral density above  $T_{\min}$  and a linear behavior in the weak-localization region, as shown in Figs. 4(b) and 4(d). A general quadratic functional form  $S_V(90 \text{ Hz}) = a_2 I^2 + a_1 I + a_0$  has been used to reproduce the  $S_V$  vs  $I$  data, in the whole investigated temperature range. Above  $T_{\min}$ , the quadratic coefficient  $a_2$  is clearly the

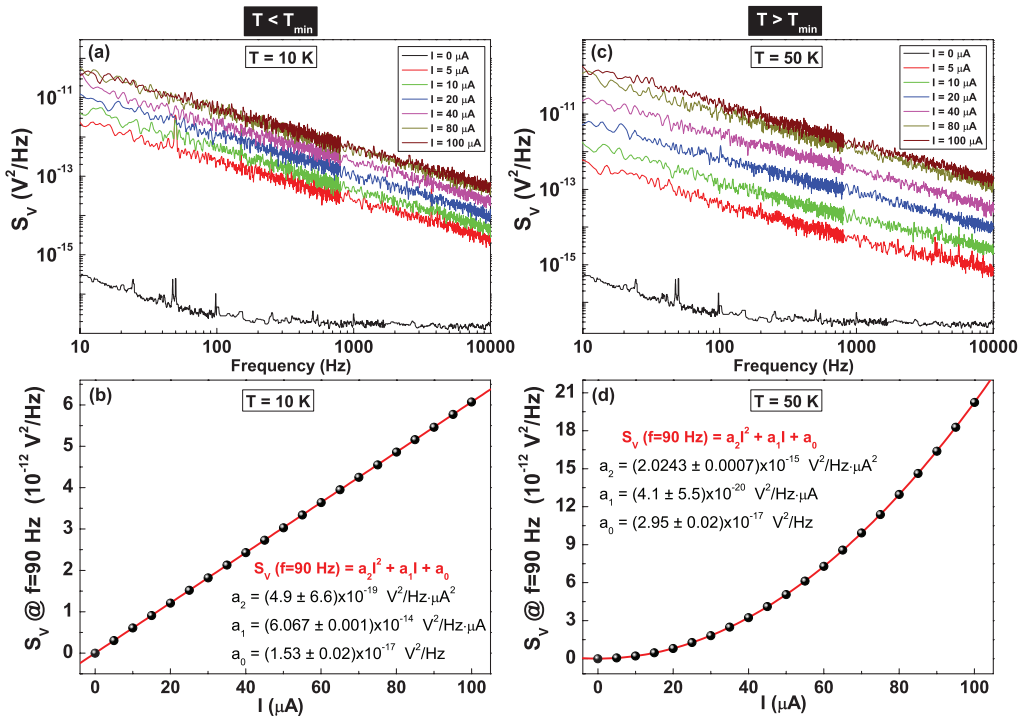


FIG. 4. (Color online) Frequency dependence of the voltage spectral density below (a) and above (c) the crossover temperature  $T_{\min}$ . Bias current dependence of  $S_V$  at a reference frequency of 90 Hz in the weak-localized,  $T = 10 \text{ K}$  (b), and metallic,  $T = 50 \text{ K}$  (d), sides. The fitting parameter values of the general quadratic functional form used are reported as insets.

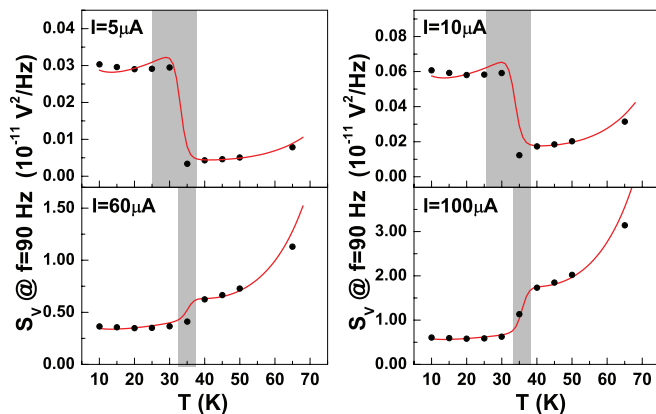


FIG. 5. (Color online) Temperature dependence of the voltage spectral density at 90 Hz and for different bias currents. The experimental data are the black dots. The model given in Eq. (7), with fitting parameters  $\chi = 0.012 \sim 20L_\Phi/L$ ,  $c_1 = 70$ , and  $c_2 = 8.478 \text{ K}^{-1}$ , is shown as a solid red line.

dominant term [see the parabolic dependence in Fig. 4(d)], thus confirming resistance fluctuations as the origin of the noise. The parameter  $a_2$  is strongly suppressed going from the metallic to weak-localization regime, while a new noise contribution  $a_1$ , linear in bias current, arises below  $T_{\min}$  [see the linear dependence in Fig. 4(b)]. The coefficient  $a_0$  originates from frequency-independent noise contributions and matches well with the temperature dependence of the sample Johnson noise.

#### IV. DISCUSSION

The spectral density model given in Eq. (7) has been compared with the experimental data. Taking  $\mathcal{C}$  and  $\chi$  as fitting parameters, a semiquantitative agreement is found. However, the proportionality factor  $\mathcal{C}$  depends on the number of fluctuators  $n_s(T)$  contributing to the noise at a given temperature. A linear dependence  $n_s(T) \propto T$  is usually reported at low  $T$ .<sup>12</sup> The latter behavior suggests that we model the temperature evolution of  $\mathcal{C}$  according to the relation  $\mathcal{C}(T) = c_1 + c_2 T$ , while the parameter  $\chi$  is assumed to be temperature independent in order to reduce the number of fitting parameters.

The resulting model is fully determined by setting  $c_{1,2}$  and  $\chi$ . The fitting procedure allows us to estimate these quantities and to interpolate the data over the whole temperature and current ranges. In Fig. 5 the theoretical model (fitting parameters  $\chi = 0.012 \sim 20L_\Phi/L$ ,  $c_1 = 70$ , and  $c_2 = 8.478 \text{ K}^{-1}$ ) is compared with the experimental data by fixing the current values to 5, 10, 60, and 100  $\mu\text{A}$ . The model reproduces the noise behavior above and below  $T_{\min}$ , while in the transition region (shaded area) a good agreement is observed only at high current values. Indeed, in this transition region the competition between WL and metallic regimes produces nonstationary fluctuations whose behavior is not captured by the model. At higher current values, however, the energy scale  $eV_\Phi$  is bigger than the thermal energy, and a bias-induced dephasing dominates the noise properties. In the latter condition the energy scales involved in the experiment are well separated, resulting in a good agreement with the model (which is based

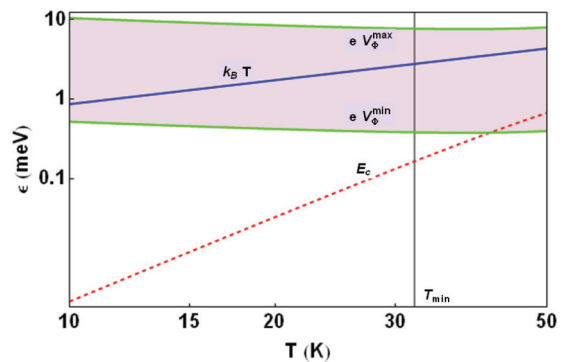


FIG. 6. (Color online) Energy scales involved in the electronic transport of the LBMO system. The bias energies  $eV_\Phi^{\min}$  and  $eV_\Phi^{\max}$  are computed fixing  $\chi \approx 0.012 \sim 20L_\Phi/L$  and taking  $I = 5 \mu\text{A}$  and  $I = 100 \mu\text{A}$ , respectively. The remaining model coefficients are fixed as  $L = 0.5 \times 10^{-3} \text{ m}$ ,  $L_\Phi = \lambda L T^{-p/2}$  [ $\lambda$  being fixed by the condition  $L_\Phi(T = 10 \text{ K}) = 0.5 \mu\text{m}$ , and  $p \simeq 3.22$ ],  $\mathcal{D} = (\hbar k_F \ell)/2m$ , and  $k_F \ell \approx 4.3$ .

on a sudden switching between the noise mechanisms above and below  $T_{\min}$ ). At high temperature ( $T \approx 65 \text{ K}$ ) the model shows a small positive deviation from the experimental data. Such a deviation is determined by the assumption  $\mathcal{C}(T) = c_1 + c_2 T$  which is invalidated by a saturation effect of  $n_s(T)$  at high temperature. The description of the saturation effect would require the inclusion of an additional free parameter in the model which is an unnecessary complication of the minimal model proposed.

In Fig. 6 the energy scales are shown as reconstructed by the fitting procedure described above. As expected, in the temperature range here considered, the applied bias represents a relevant dephasing source ( $eV_\Phi^{\min, \max} > E_c$ ), thus providing a validation of the model assumptions. However, in order to observe bias-dependent effects on the noise signal, the WL regime is required. This statement is justified by the following argument.

In a generic coherent box the Hamiltonian is  $H = H_0 + eV_\Phi$ , while the associated electron wave function is given by  $\psi(t_f) = \psi_0 \exp(-i \int_{t_i}^{t_f} dt eV_\Phi/\hbar)$ ,  $\psi_0$  being associated with the Hamiltonian  $H_0$ . The phase memory is limited by the phase relaxation time  $\tau_\Phi \sim \tau_D = L_\Phi^2/\mathcal{D}$ , and thus the typical electromagnetic phase shift  $\exp(-i\delta)$  acquired by the electron traveling through a coherent box is given by  $\delta \approx \chi \frac{\Phi_0 I}{E_F} (L_\Phi/\ell)^2$ ,  $\Phi_0 = h/e$  being the flux quantum and  $E_F$  the Fermi energy. Consequently, the phase shift  $\delta$  can induce observable effects on the transport properties only in the WL regime where the condition  $L_\Phi \gg \ell$  is obeyed.

A conclusive analysis on the universality of the proposed fluctuations mechanisms should require experimental investigations of simple metals (such as gold, silver, etc). Further studies on these materials are currently in progress.

#### V. CONCLUSIONS

In conclusion, detailed voltage spectral-density measurements have been performed on different compounds, focusing the attention on LBMO thin films as the prototype system in which WL effects produce anomalous bias dependence

of the  $1/f$  noise component. The observed phenomenology appears to be reproducible in different samples and materials undergoing WL transition, calling for a common universal origin. By means of a theoretical analysis based on nonequilibrium UCFs, a simple model explaining the anomalous bias dependence of the noise has been derived. The theoretical analysis shows that the low-temperature noise ( $T < T_{\min}$ ) is mainly originated by the dephasing of the electronic paths when the condition  $V_{\phi} > E_c/e$  is satisfied, while above  $T_{\min}$  standard thermal averaging can fully explain the observed noise. The dephasing processes responsible for the observed anomalous noise behavior do not affect the weak-localization correction to the classical resistance, which involves a special subset of Feynman diagrams (time reversed), presenting a definite energy-independent phase relation. In this respect the averaging over the energy window  $\Delta E$  does not introduce any phase cancellation in the diagrams contributing to the WL corrections,<sup>19</sup> the latter being an important point in understanding the Ohmic behavior of the system (i.e., the noise is bias dependent, while the system resistance is bias independent). On the other hand, above the critical voltage  $E_c/e$ , the current bias  $I$  actively contributes to the dephasing of the electronic paths not involved in the WL correction by reducing the quantum interference terms by  $(E_c/eV_{\phi})^{1/2} \ll 1$ .<sup>10</sup> The latter information, not present in the dc transport measurements, is effectively captured by the noise

spectroscopy. As a final remark, as pointed out in Ref. 26 for quasi-one-dimensional systems at very low temperature (mK range), electron-electron scattering at high bias voltages  $V$  may induce a  $1/V$  power-law lowering of the variance of the conductance similar to the one discussed in this work. In the experimental case reported here, the phononic origin of the dephasing mechanism is observed, while at low temperature ( $T < 10$  K) an increasing relevance of the electron-electron interaction could be expected.<sup>3</sup> Although further studies are required to fully investigate nonequilibrium UCFs as an effective noise source at low temperature, the above findings shed some light on the relation between  $1/f$  noise and the quantum nature of matter at the *boundary* between classical and quantum realms.

### ACKNOWLEDGMENTS

Financial support from CNR-SPIN Seed Project “Weak Localization” is gratefully acknowledged. This work was also partially supported by the Italian MIUR Grant No. PRIN 20094W2LAY, *Ordine orbitale e di spin nelle eterostrutture di cuprati e manganiti*. A.G. acknowledges financial support of PON Ricerca e Competitività 2007-2013 under Grant Agreement No. PON NAFASSY, PONa3-00007. A.G. and A.N. acknowledge financial support from the EU VII FW Programme under Grant Agreement No. 264098 MAMA.

\*cbarone@unisa.it

†spagano@unisa.it

<sup>1</sup>P. A. Lee and T. V. Ramakrishnan, *Rev. Mod. Phys.* **57**, 287 (1985).

<sup>2</sup>B. L. Al'tshuler and D. E. Khmel'nitskiĭ, *Pis'ma Zh. Eksp. Teor. Fiz.* **42**, 291 (1985) [*JETP Lett.* **42**, 359 (1985)].

<sup>3</sup>S. Wind, M. J. Rooks, V. Chandrasekhar, and D. E. Prober, *Phys. Rev. Lett.* **57**, 633 (1986).

<sup>4</sup>S. Kar, A. K. Raychaudhuri, A. Ghosh, H. v. Löhneysen, and G. Weiss, *Phys. Rev. Lett.* **91**, 216603 (2003).

<sup>5</sup>D. Neumaier, K. Wagner, U. Wurstbauer, M. Reinwald, W. Wegscheider, and D. Weiss, *New J. Phys.* **10**, 055016 (2008).

<sup>6</sup>D. S. Golubev and A. D. Zaikin, *New J. Phys.* **10**, 063027 (2008).

<sup>7</sup>C. Barone, A. Guarino, A. Nigro, A. Romano, and S. Pagano, *Phys. Rev. B* **80**, 224405 (2009).

<sup>8</sup>M. Ziese, *Phys. Rev. B* **68**, 132411 (2003).

<sup>9</sup>T. Okuda, T. Kimura, and Y. Tokura, *Phys. Rev. B* **60**, 3370 (1999).

<sup>10</sup>R. A. Webb and S. Washburn, *Phys. Today* **41**(12), 46 (1988).

<sup>11</sup>S. Feng, P. A. Lee, and A. D. Stone, *Phys. Rev. Lett.* **56**, 1960 (1986); **56**, 2772 (1986).

<sup>12</sup>N. O. Birge, B. Golding, and W. H. Haemmerle, *Phys. Rev. Lett.* **62**, 195 (1989).

<sup>13</sup>G. A. Garfunkel, G. B. Alers, M. B. Weissman, J. M. Mochel, and D. J. VanHarlingen, *Phys. Rev. Lett.* **60**, 2773 (1988).

<sup>14</sup>C. Terrier, D. Babić, C. Strunk, T. Nussbaumer, and C. Schönenberger, *Europhys. Lett.* **59**, 437 (2002).

<sup>15</sup>B. Savo, C. Barone, A. Galdi, and A. Di Trolio, *Phys. Rev. B* **73**, 094447 (2006).

<sup>16</sup>S. Cox, J. Singleton, R. D. McDonald, A. Migliori, and P. B. Littlewood, *Nat. Mater.* **7**, 25 (2008).

<sup>17</sup>S. Kogan, *Electronic Noise and Fluctuations in Solids* (Cambridge University Press, Cambridge, 1996).

<sup>18</sup>Y. Imry, *Introduction to Mesoscopic Physics* (Oxford University Press, New York, 2002).

<sup>19</sup>P. A. Lee, A. D. Stone, and H. Fukuyama, *Phys. Rev. B* **35**, 1039 (1987).

<sup>20</sup>G. Neuttiens, C. Strunk, C. Van Haesendonck, and Y. Bruynseraede, *Phys. Rev. B* **62**, 3905 (2000).

<sup>21</sup>P. Orgiani, R. Ciancio, A. Galdi, S. Amoroso, and L. Maritato, *Appl. Phys. Lett.* **96**, 032501 (2010).

<sup>22</sup>C. Barone, A. Galdi, S. Pagano, O. Quaranta, L. Méchin, J.-M. Routoure, and P. Perna, *Rev. Sci. Instrum.* **78**, 093905 (2007).

<sup>23</sup>P. Orgiani, C. Adamo, C. Barone, A. Galdi, A. Yu. Petrov, D. G. Schlom, and L. Maritato, *Phys. Rev. B* **76**, 012404 (2007).

<sup>24</sup>E. Rozenberg, M. Auslender, I. Felner, and G. Gorodetsky, *J. Appl. Phys.* **88**, 2578 (2000).

<sup>25</sup>Qing'An Li, K. E. Gray, and J. F. Mitchell, *Phys. Rev. B* **63**, 024417 (2000).

<sup>26</sup>T. Ludwig, Ya. M. Blanter, and A. D. Mirlin, *Phys. Rev. B* **70**, 235315 (2004).